



Article

Change of Human Footprint in China and Its Implications for Carbon Dioxide (CO₂) Emissions

Yuan Li ^{1,2}, Wujuan Mi ², Yuheng Zhang ², Li Ji ¹, Qiusheng He ³ , Yuanzhu Wang ⁴ and Yonghong Bi ^{2,*} ¹ School of Environment and Resources, Taiyuan University of Science and Technology, Taiyuan 030024, China² State Key Laboratory of Freshwater Ecology and Biotechnology, Institute of Hydrobiology, Chinese Academy of Sciences, Wuhan 430072, China³ Institute of Intelligent Low Carbon and Control Technology, Taiyuan University of Science and Technology, Taiyuan 030024, China⁴ Central Southern Safety & Environmental Technology Institute Company Limited, Wuhan 430072, China

* Correspondence: biyh@ihb.ac.cn; Tel.: +86-27-68780016

Abstract: Humans have altered the earth in unprecedented ways, and these changes have profound implications for global climate change. However, the impacts of human pressures on carbon dioxide (CO₂) emissions over long time scales have not yet been clarified. Here, we used the human footprint index (HF), which estimates the ecological footprint of humans in a given location, to explore the impacts of human pressures on CO₂ emissions in China from 2000 to 2017. Human pressures (+13.6%) and CO₂ emissions (+198.3%) in China are still on the rise during 2000–2017 and are unevenly distributed spatially. There was a significant positive correlation between human pressures and CO₂ emissions in China, and northern China is the main driver of this correlation. The increase of CO₂ emissions in China slowed down after 2011. Although human pressures on the environment are increasing, high-quality development measures have already had noticeable effects on CO₂ emission reductions.

Keywords: carbon dioxide emissions; global climate change; human footprint index; human pressures; macro control



Citation: Li, Y.; Mi, W.; Zhang, Y.; Ji, L.; He, Q.; Wang, Y.; Bi, Y. Change of Human Footprint in China and Its Implications for Carbon Dioxide (CO₂) Emissions. *Remote Sens.* **2023**, *15*, 426. <https://doi.org/10.3390/rs15020426>

Academic Editor: Ashraf Dewan

Received: 21 November 2022

Revised: 3 January 2023

Accepted: 4 January 2023

Published: 10 January 2023



Copyright: © 2023 by the authors. Licensee MDPI, Basel, Switzerland. This article is an open access article distributed under the terms and conditions of the Creative Commons Attribution (CC BY) license (<https://creativecommons.org/licenses/by/4.0/>).

1. Introduction

Humans have been reshaping the world for millennia. The current geological epoch has been renamed the “Anthropocene” [1] because of the major environmental impacts associated with human activities, especially the conversion of large-scale natural habitats to cropland and the construction of land to feed and house our burgeoning population [2]. Human activities affect the stability of ecosystems and have a multitude of deleterious effects on the environment, including nutrient pollution [3]; modifications of land surface hydrology [4]; loss of the productivity, composition, and diversity of terrestrial ecosystems [5]; introduction of alien species; and alterations of the biogeochemical cycles of carbon [6]. Scientists have expressed much concern over the extent of human-induced environmental destruction, which is rapidly approaching catastrophic levels.

As a consequence of the cumulative impacts of anthropogenic activities on the planet in recent decades, the concentrations of greenhouse gases including carbon dioxide (CO₂), methane (CH₄), and nitrous oxide (N₂O), have been continuously increasing [7]. The accumulation of greenhouse gases prevents the loss of heat from the earth and increases the temperature of the earth’s surface, which results in an increase in the frequency and intensity of extreme weather events, including drought, flood, heat waves, and freezing stress [8,9]. The 2015 Paris Agreement ambitiously aims to limit warming to between 1.5 °C and 2 °C by mid-century, which will require achieving a balance between anthropogenic emissions and the removal of longer-lived greenhouse gases such as CO₂ [10]. Many

countries, such as China and the United States, have made net-zero pledges and have started to reduce emissions [11].

The extent and intensity of anthropogenic changes are spatially heterogeneous. Many anthropogenic pressures, such as population growth, fossil fuel combustion, industrial emissions, agricultural production, livestock farming, and land-use change, can interact in diverse ways [12,13]. Currently used mapping approaches often fail to capture many lower-intensity forms of human pressures, such as our extensive networks of roads, grazing lands, and low-density human settlements, the effects of which are more insidious than outright habitat conversion [14]. For example, land-use cover has major effects on the global extent and distribution of terrestrial carbon emissions [15]. Changes in land-use type from high-vegetation to low-vegetation biomass usually result in carbon emissions; land-use management, such as measures to control wildfires, pests, and diseases, can also affect carbon storage. Land-use change and management have together been estimated to contribute approximately one-third of all anthropogenic carbon emissions since the industrial revolution [16,17]. Non-settlement areas can also potentially result in population displacement and enrichment [2]; however, the role of low stress factors on the environment is often ignored in such areas. A comprehensive human stress indicator of multiple factors for studying the spatiotemporal patterns of CO₂ emissions is often more effective for characterizing regions with high emissions [18]. Furthermore, key variables, including technology, infrastructure, environment and finance, have important practical significance in achieving carbon neutrality [19–21]. For example, Labzovskii et al., (2017) [22] have projected that a beneficial policy would result in 24%, 80%, 166% less CO₂ emissions in East Asia by 2020, 2025 and 2030, respectively.

Improvements in remote sensing geographic data and geographic information systems permit the construction of detailed maps displaying human activities, such as the human footprint index (HF) [23]. HF captures the total ecological footprint of the human population in a given location [24]. Venter et al., constructed a global human footprint map from 1993 to 2009 and found that intense human pressures have had significant effects on native biodiversity [25]. This study also revealed that environmental pressures were lower in the wealthiest countries. A series of studies have also shown that human activities have had substantial effects on marine and lake ecosystems through the construction of human footprint maps [26,27]. However, the macro-scale effects of human pressures on CO₂ emissions have not yet been thoroughly studied.

China has experienced rapid economic development since its reform and opening in the late 1970s, which has resulted in the emission of large amounts of CO₂. A better understanding of spatiotemporal patterns in human pressures and their effects on CO₂ emissions is needed to respond to calls for rapid action to limit CO₂ emissions. Here, we used the latest multi-source remote sensing data to quantify the effects of human pressures on China's regional and sectoral CO₂ emissions between 2000 and 2017. Remote sensing data on (1) land-use cover, (2) roads, (3) railways, (4) human population density, (5) grazing density, and (6) night-time lights were used. We explored the spatiotemporal dynamics in human pressures and CO₂ fluxes and analyzed the correlations between human pressures and CO₂ fluxes. Our results reveal that CO₂ emissions in China have been on the rise from 2000 to 2017 and that there is a strong correlation between CO₂ emissions and human pressures. Nevertheless, increases in CO₂ emissions have slowed down after 2011, indicating that the effects of high-quality development and national measures to reduce greenhouse gas emissions have started to have impacts on CO₂ emission reductions.

Our results enhance the understanding of the impacts of human pressures on the environment and have implications for the formulation of effective and environmentally friendly strategies. The results have a positive guiding significance for carbon emission reduction policies, including urban land planning, population size control, industrial structure optimization, industrial technology upgrading, etc. In this paper, Section 2 provides a brief overview of the study methods, data sources, and model construction. Then, the spatio-temporal characteristics of HF and CO₂, and their correlation analysis

during 2000–2017 in China are provided in Section 3. The cause of spatial distribution of HF and CO₂, and the response and driving factors of CO₂ emissions to human pressure changes are discussed in Section 4. Finally, Section 5 outlines the potential extension, outlook, and the summary of this study.

2. Methods and Data

2.1. Overview

The human footprint (HF) is a global map of human influence on the land surface [28]. The human footprint can reflect human disturbance to the natural environment and is directly or indirectly related to human fossil fuel combustion, fertilizer use, and industrial activity, thus establishing a certain relationship with CO₂ emissions [29]. We used the HF for data from 2000 to 2020 to facilitate comparison across human pressures. The human pressures considered were (1) land-use cover, (2) roads, (3) railways, (4) human population density, (5) night-time lights, and (6) grazing density. We performed buffer analysis and assigned scores ranging from 0 to 10 to various spatial data layers according to the intensity of each human pressure; the assigned layers were then overlaid and normalized by partitioning to obtain human footprint data that indicate the extent of terrestrial human activity. We used ArcGIS 10.2 to integrate spatial data on human pressures at the 1 km² resolution for China's land areas. For any grid cell, the human footprint ranged between 0 and 60. We classified HF into three categories to reflect the degree of human pressures: low (HF < 20), moderate (HF 20–30), and high (HF 30–60).

2.2. Land-Use Cover

Change in land-use cover reflects the long-term impact of human activities on the environment [30]. Anthropogenic land-use cover change has a pronounced effect on regional climate change [31]. For example, land-use change (e.g., deforestation, increases in cropland, livestock rearing, and urban and industrial land expansion) and land management (wildfires, pests, and diseases) can directly or indirectly increase CO₂ emissions, especially in developing and poor countries [32–35]. Overall land-use change and land management have contributed approximately 1.45 Pg of the total carbon released from 1990 to 2010 [36]. We downloaded the database files of land-use cover (accurate to 1 km) from the Resource and Environment Science and Data Center (<http://www.resdc.cn/>, accessed on 1 January 2022). We assigned a pressure score of 10 to construction land, 7 to agricultural land, 4 to grasslands, and 0 to all other types of land-use cover. We used the land-use cover data of 2000, 2005, 2010, 2015, and 2020 to approximate the data for 2000–2003, 2004–2007, 2008–2011, 2012–2015, and 2016–2017, respectively.

2.3. Roads and Railways

Transport infrastructure is a fundamental physical foundation of societies; it thus plays a key role in supporting socio-economic activities and affects both the local and global environment [37,38]. Road transport contributes more than 60% of the CO₂ emissions of all transport activities [39], and a unidirectional causality has been noted between railway infrastructure and energy consumption [40]. An increasing number of transport infrastructure projects have been implemented in newly urbanizing regions.

We acquired data on the distribution of roads and railways for the years 2000, 2005, 2010, and 2012–2017 from OpenStreetMap. The OpenStreetMap database represents the most comprehensive publicly available database on roads and railways. We excluded all trails and private roads and used provincial major highways to denote roads. We used the road network data of 2000, 2005, and 2010 to approximate the data for 2000–2003, 2004–2007, and 2008–2011, respectively. We evaluated the direct and indirect pressures of roads by designating a pressure score of 10, 8, and 4 for 0.5, 0.5–1.5, and 1.5–2.5 km of distance on either side of the roads. The direct pressure of railways was assigned a score of 8 for a distance of 0.5 km on either side of them.

2.4. Population Density

Population density is an important indicator of the intensity of the interaction between human activities and ecosystems, and there is a strong correlation between population density and CO₂ emissions. Population density has significant positive effects on increases in CO₂ emissions. A previous study has shown that population density increases of 1% lead to total net CO₂ emissions increases of 4% [41,42].

Population density was mapped using the gridded population data published by WorldPop. The data set provides a 1 km × 1 km gridded summary of population census data from 1990 to 2017. Random forest-based asymmetric redistribution was used for mapping. The impact of population density on ecosystems is logarithmic. The population density data were assigned a pressure score ranging from 0 to 10. The maximum value of population density was 366,587 persons/km², and the population density pressure score was logarithmically scaled using the following formula:

$$\text{Population score} = 2.21398 \times \log(\text{Population density} + 1) \quad (1)$$

2.5. Grazing Density

Overgrazing (i.e., heavy grazing) associated with the rapid sharp growth of the human population and food demand in recent years is a major contributor to increases in greenhouse gas fluxes [43].

We tallied the number of large livestock animals, including cattle, horses, donkeys, mules, and camels, kept in each provincial administrative region of China using information published by the National Bureau of Statistics of China from 2000 to 2017. The impact of grazing density on ecosystems is logarithmic. The grazing density data were assigned a pressure score of 0–10. The maximum value of grazing density was 93.327 heads/km² (calculated by provincial administrative unit), and the grazing density pressure score was logarithmically scaled using the following formula:

$$\text{Livestock score} = 2.51531 \times \log(\text{grazing density} + 1) \quad (2)$$

2.6. Night-Time Lights

Night-time light satellite imagery is correlated with socioeconomic parameters such as urbanization, economic activity, and population density [44–46]. Night-time light imagery of 2000–2013 was obtained from the Defense Meteorological Satellite Program–Operational Linescan System (DMSP–OLS). The night-time light imagery of 2014–2020 was obtained from the launch of the NASA/NOAA’s Suomi—Visible Infrared Imaging Radiometer Suite (VIIRS) sensor.

We used the annual mean synthesis algorithm without the effect of moonlight and cloud cover, and the spatial resolution of the images was 1 km × 1 km. Because of the lack of in-orbit radiometric calibration and correction facilities, the nocturnal radiometric signals on all light images were discretized into digitized radiometric brightness values (hereafter referred to as DN values, with scores ranging from 0 to 63). The synthetic product of this series of stable night-light signals eliminates the effect of short-time radiation sources so that the parts covered by the high brightness DN values usually correspond to high-density human settlements and activities. DN values of 8 or less were excluded from consideration before inter-calibration of data, as the shape of the quadratic function leads to severe distortion of very low DN values. The inter-calibrated DN data were then rescaled using an equal quintile approach into a 0–10 scale.

2.7. CO₂ Fluxes

The emission inventory of CO₂ fluxes was obtained from the latest energy data revision (2015) of the China National Bureau of Statistics from Scientific Data (<https://doi.org/10.6084/m9.figshare.c.5136302.v2>, accessed on 1 January 2022) [47,48]. The carbon emission unit is accurate to the county administrative region. We collected data on the CO₂ emissions

of 2689 county-level administrative regions in China from 2000 to 2017 (Figure S1). The CO₂ emission fluxes were classified into three categories: low (0–10 Mt), moderate (10–30 Mt), and high (30–60 Mt).

2.8. Statistical Analyses

We performed all simple linear regression analysis, including the determination of 95% confidence intervals, with SigmaPlot 14.0 (Systat Software, San Jose, CA, USA). r^2 indicates the fit of a one-dimensional linear regression, and $p < 0.0001$ was the threshold for statistical significance. Standard deviations of CO₂ emissions and HF by different regions were calculated using SigmaPlot 14.0 software. We evaluated bivariate comparisons of continuous data measurements using analysis of variance (ANOVA) tests. CO₂ emissions and HF by different regions were expressed as average and standard error (SE). We tested the errors of HF calculation using a Monte Carlo simulation with 1000 iterations. We used histograms, conducted linear regressions, and built line plots. We used Origin Pro 2021 (Microcal Software, Seattle, WA, USA) to make violin plots and stacked area plots. All the spatial patterns of CO₂ emissions and HF in China were analyzed by ArcGIS 10.2 (ESRI, Redlands, CA, USA) [49].

3. Results

3.1. Spatio-Temporal Pattern of Human Footprint in China

HF in China was mainly concentrated in the 0–20 range, spanning 482×10^4 km² (Figure 1a). The area of high (30–60), moderate (20–30), and low HF (0–20) in China was 5.53×10^4 km², 100.11×10^4 km², and 684.09×10^4 km², respectively (Table S1). There was high spatial variation in HF (Figure 2a; Figure S2). The largest and smallest areas of high HF were observed in eastern (1.57×10^4 km²) and northwestern China (0.22×10^4 km²) during 2000–2017. The mean HF in China was 20.89 and gradually increased from 19.84 in 2000 to 22.54 in 2017 (Table 1; Figure 1b). HF in China increased 13.6% during 2000–2017. The rate of change of HF was the highest (16.87%) and the lowest (9.63%) in southern and northern China, respectively (Table 2). The area of low HF was 699.50×10^4 in 2000 and 645.05×10^4 km² in 2017 (a decrease of 7.78%), and the area of high HF was 2.66×10^4 in 2000 and 12.84×10^4 km² in 2017 (an increase of 382.71%) (Table S1). The area of high HF was 0.07×10^4 in 2000 and 0.99×10^4 km² in 2017 (an increase of 1314.29%), and the area of high HF was 0.67×10^4 in 2000 and 1.97×10^4 km² in 2017 (an increase of 194.03%). Some of the low HF areas were converted into high HF areas (Table S1; Figure 3).

Table 1. Average human footprint index in different regions of China during 2000–2017.

Region/Human Footprint	Nationwide	North	South	Northeast	Northwest	Southwest	Central	East
2000	19.84	22.22	17.75	20.04	15.60	17.51	21.10	22.96
2001	20.30	22.62	18.25	20.50	15.86	17.97	21.60	23.56
2002	20.39	22.71	18.32	20.60	15.89	18.07	21.72	23.62
2003	20.30	22.57	18.23	20.52	15.86	18.01	21.57	23.58
2004	20.66	22.99	18.72	20.89	16.07	18.16	21.82	24.22
2005	20.51	22.91	18.48	20.79	16.08	18.12	21.74	23.76
2006	20.59	22.94	18.56	20.73	16.14	18.14	21.78	24.09
2007	20.62	22.89	18.61	20.84	16.14	18.20	21.82	24.07
2008	21.00	23.18	19.53	21.20	14.68	17.26	22.32	26.65
2009	20.36	22.45	18.15	21.52	15.94	18.03	21.40	23.58
2010	20.80	22.83	18.58	21.82	16.20	18.28	21.93	24.41
2011	20.62	22.58	18.56	21.53	16.14	18.13	21.77	24.13
2012	20.66	22.63	18.62	21.55	16.15	18.11	21.77	24.28
2013	21.01	23.01	19.08	21.82	16.42	18.26	22.13	24.80
2014	21.76	23.56	19.89	22.44	17.17	19.18	22.92	25.58
2015	21.94	23.75	20.05	22.45	17.39	19.47	23.10	25.73
2016	22.06	23.86	20.23	22.40	17.47	19.60	23.28	25.84

Table 1. Cont.

Region/Human Footprint	Nationwide	North	South	Northeast	Northwest	Southwest	Central	East
2017	22.54	24.36	20.75	22.61	17.95	20.17	23.78	26.38
Mean	20.89	23.00	18.91	21.35	16.29	18.37	22.08	24.51
Increment	2.70	2.14	3.00	2.56	2.36	2.67	2.68	3.43
Chang rate (%)	13.60	9.63	16.87	12.79	15.10	15.22	12.70	14.93

Table 2. Average CO₂ emissions in different regions of China during 2000–2017.

Region/CO ₂ (Mt)	Nationwide	North	South	Northeast	Northwest	Southwest	Central	East
2000	3194.81	667.21	356.84	400.53	229.78	330.06	476.33	734.06
2001	3217.34	669.42	350.19	386.20	226.75	319.82	461.73	803.24
2002	3479.13	719.42	381.91	421.16	243.48	352.55	507.16	853.46
2003	4096.50	837.24	450.23	485.05	281.49	411.74	590.76	1039.99
2004	4563.96	938.00	495.90	528.05	312.21	451.57	649.31	1188.92
2005	5436.70	1146.47	566.70	599.41	376.44	519.93	755.62	1472.13
2006	6108.38	1288.76	633.53	666.01	428.81	583.65	852.48	1655.14
2007	6531.10	1392.01	676.34	696.40	463.74	609.99	906.38	1786.25
2008	6998.28	1517.54	718.40	728.45	515.83	644.30	969.04	1904.71
2009	7544.90	1624.49	775.05	798.30	562.53	707.13	1050.15	2027.24
2010	8255.42	1797.20	842.24	857.27	645.66	775.00	1153.96	2184.08
2011	9203.94	2034.41	956.37	880.08	836.84	855.11	1326.43	2314.70
2012	9392.04	2070.30	976.45	905.84	846.57	877.53	1354.86	2360.50
2013	9435.14	2040.80	992.97	942.87	932.23	884.33	1379.38	2262.56
2014	9627.14	2060.61	1019.12	958.79	955.57	905.33	1408.05	2319.68
2015	9094.56	1955.65	962.94	903.13	884.74	837.85	1316.03	2234.21
2016	9370.32	1955.91	995.40	934.62	907.05	863.46	1355.86	2318.02
2017	9531.09	1998.36	1022.76	904.80	999.15	909.80	1395.81	2300.41
Accumulated value	125,081	26,714	13,173	12,997	10,649	11,839	17,909	31,759
Increment	6336	1331	666	504	769	580	919	1566
Chang rate (%)	198.33	199.51	186.61	125.90	334.83	175.65	193.03	213.38

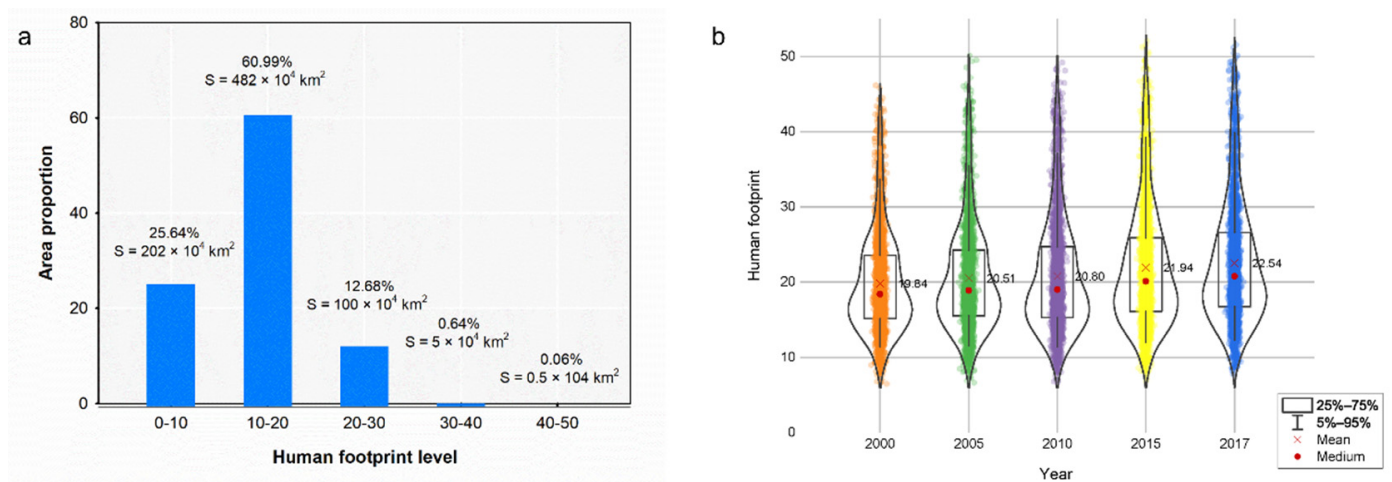


Figure 1. Cont.

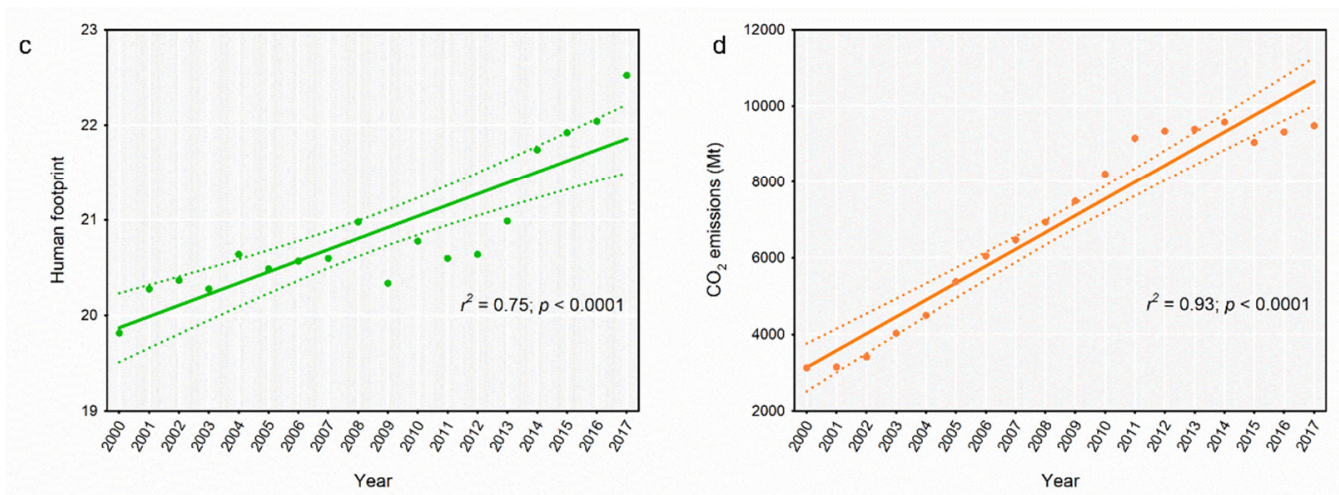


Figure 1. Features of human footprint and CO₂ emissions in China including (a) area of different human footprint classes, (b) variation in the average human footprint in different years, (c) regression analysis of human footprint and time, and (d) regression analysis of CO₂ emissions and time.

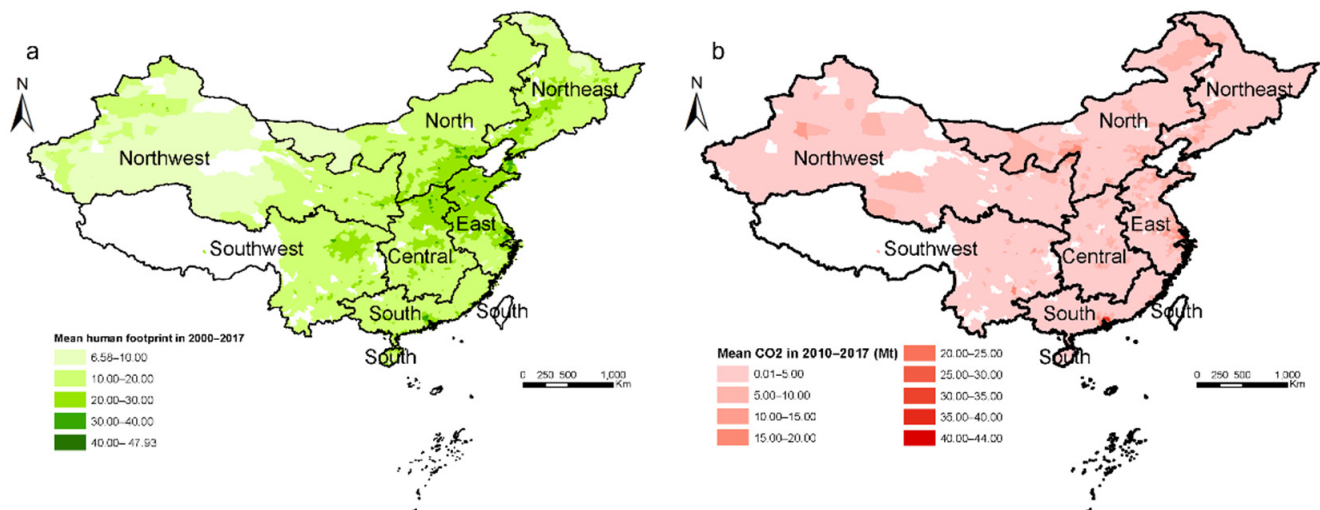


Figure 2. Spatial pattern of the average (a) human footprint and (b) CO₂ emissions in different regions in China during 2000–2017.

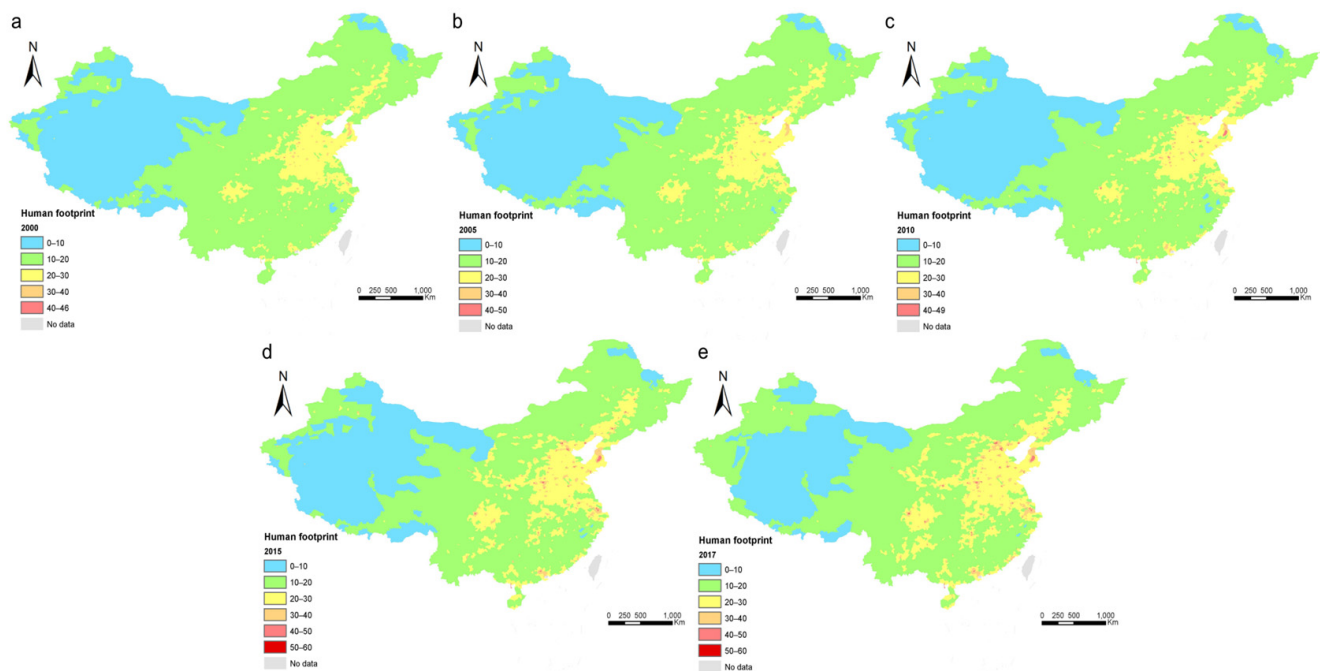


Figure 3. Spatio-temporal pattern of human footprint in China in (a) 2000, (b) 2005, (c) 2010, (d) 2015, and (e) 2017.

3.2. Spatio-Temporal Dynamics of CO₂ Emission Fluxes in China

China emitted a total of 125,081 Mt CO₂ during 2000–2017 (Table 2). CO₂ emissions in China gradually increased from 3194.81 in 2000 to 9531.09 Mt in 2017 (an increase of 198.33%). There was pronounced spatial variation in CO₂ emission fluxes in different regions (Figure 2b). CO₂ emissions contributed by eastern and northwestern China were the highest (31,759 Mt) and lowest (11,839 Mt), respectively (Table 2; Figure 4). CO₂ emission fluxes in China increased by 6336 Mt; the largest increase was observed in eastern China (1556 Mt), and the lowest increase was observed in northeastern China (504 Mt). CO₂ emissions in all regions of China increased by more than 100%. The rate of change in CO₂ emissions for northwestern (334.83%), eastern (213.38%), and northern China (199.51%) exceeded the national average (Table 2). The high (30–60), moderate (10–30), and low (0–10) CO₂ emissions in China increased 122.05, 1625.53, and 4588.70 Mt, respectively (Table S2; Figure S3). The high CO₂ emissions in southern (44.03 Mt) and eastern China (43.77 Mt) increased the most. Some of the low CO₂ emission areas were converted into high CO₂ emission areas (Table S2; Figure 5). CO₂ emissions were shown to have peaked in 2011 (+948.52 Mt) and were lowest in 2015 (−532.58 Mt) (Figure 6a). There was a gradual decrease in the magnitude of the increases of average CO₂ emissions in China during 2000–2017.

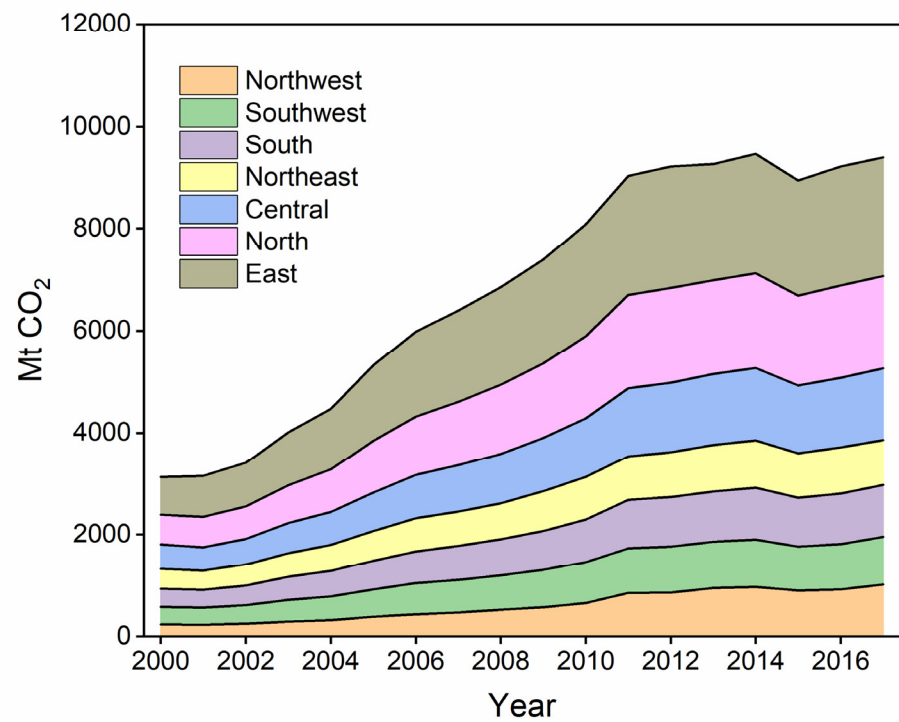


Figure 4. Stacked area map of annual CO₂ emissions in different regions in China during 2000–2017.

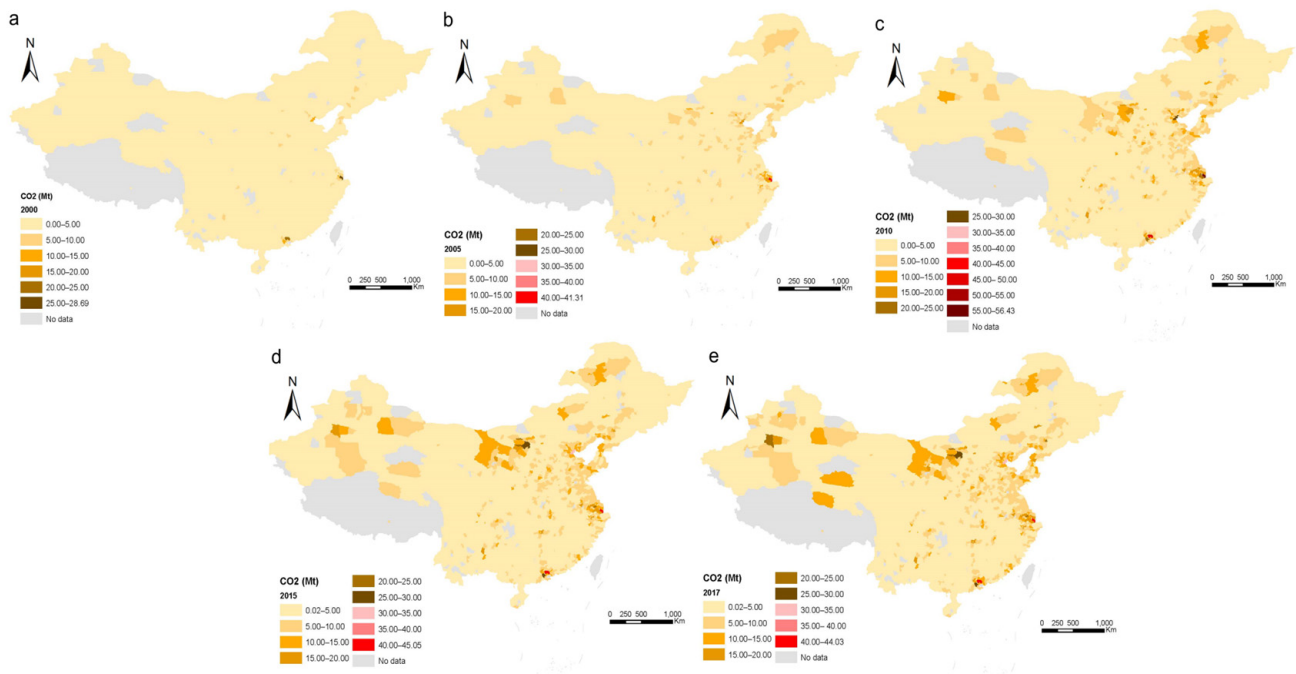


Figure 5. Spatio-temporal pattern of CO₂ emissions in China in (a) 2000, (b) 2005, (c) 2010, (d) 2015, and (e) 2017.

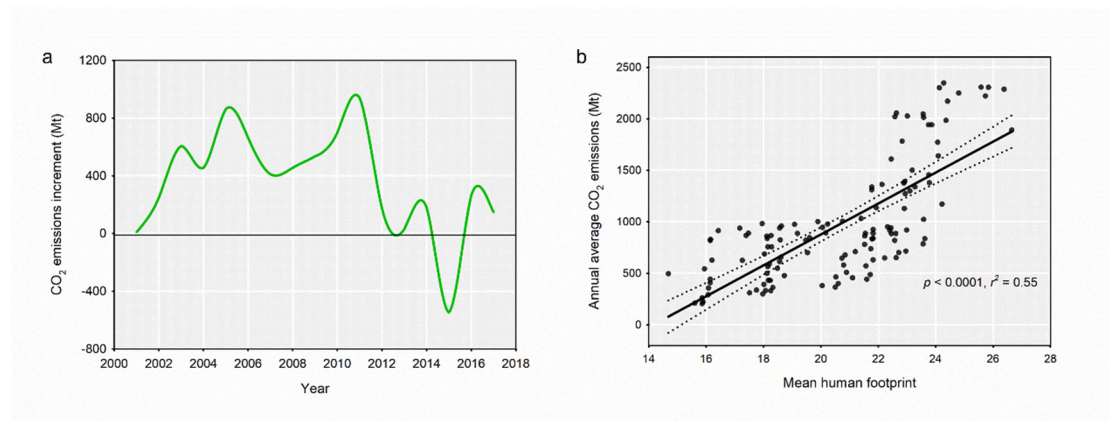


Figure 6. Trends in the (a) annual increase in CO₂ emissions and the (b) relationship between the average human footprint and average annual CO₂ emissions.

CO₂ emissions were higher in the provinces of Shandong (577.08 Mt y⁻¹), Jiangsu (497.00 Mt y⁻¹), and Hebei (492.35 Mt y⁻¹), which accounted for 23% of total emission fluxes in China (Figure S4). Global Moran's *I* was calculated to measure the spatial autocorrelation in CO₂ emissions. Its value was 0.14 ($p < 0.01$), which indicates a significant positive spatial autocorrelation in CO₂ emissions. The local Moran's *I* was used to further study the spatial characteristics of CO₂ emissions in 2000 (Figure 7a) and 2017 (Figure 7b) in China. There was a significant expansion of high-high cluster areas from 2000 to 2017, especially into eastern and northern China. The low-low cluster areas were mainly located in southwest China.

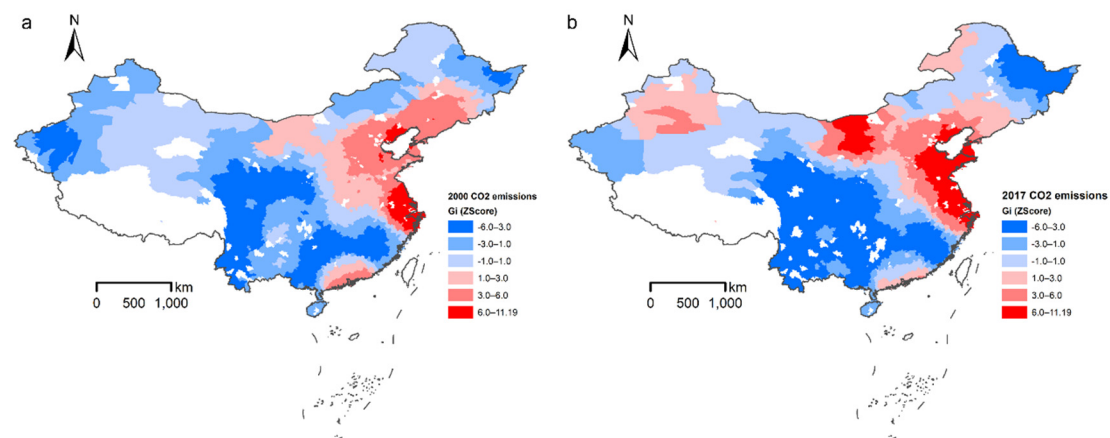


Figure 7. Spatial autocorrelation analysis (local Moran's *I* clustering) of CO₂ emissions in China in (a) 2000 and (b) 2017. Red and blue areas indicate positive and negative spatial correlation, respectively.

3.3. Correlations between CO₂ Emissions and Human Pressures

HF and CO₂ emissions in different regions of China were significantly positively correlated based on a Spearman's correlation coefficient for ranked data (correlation coefficient = 0.49, $p < 0.0001$) (Figure 6b). HF ($n = 18$; $r^2 = 0.75$; $p < 0.0001$) and CO₂ emissions ($n = 18$; $r^2 = 0.93$; $p < 0.0001$) in China increased significantly over time during the period 2000–2017 (Figure 1c; Figure 1d). The HF was highest (24.51) and lowest (16.29) in eastern and northwestern China, respectively (Table 2). CO₂ emissions were highest (1484 Mt) and lowest (592 Mt) in eastern and northwestern China, respectively (Table 2). During this 18-year period, the annual CO₂ emissions in each region were significantly positively correlated with HF ($n = 126$; $r^2 = 0.55$; $p < 0.0001$).

4. Discussion

4.1. Characteristics of Human Pressures in China

The human footprint provides a spatially explicit and temporally consistent quantitative measure of the magnitude of human pressures on the environment. Human pressures alter natural environments and harm natural systems [50]. These pressures include land-use cover (e.g., agricultural land and construction land), transportation (e.g., roads, railways, and navigable waterways), agricultural land and construction land, and trade (e.g., imports, exports, and international exports of energy-intensive industries) [51]. Human pressures (indicated by HF) could also be frequent, small in magnitude, and thus overlooked, such as the effects of extensive road systems and pasture lands. Spatial patterns of HF and human pressures were closely related. China has been the world's second largest economy since 2010. Spatial heterogeneity in regional human activities leads to spatial heterogeneity in human pressures in China. Eastern China is located between the mainland and the sea; it is characterized by gentle terrain and features agriculturally productive soils. In addition, this region is rich in aquatic products, oil, iron ore, salt, and other resources, the labor force is large, and the industrial and agricultural base is strong. By the end of 2017, eastern China accounted for only 5.25% of the country's area, but 23.28% of its population, 32.70% of its GDP, 32.99% of its road area, and 33.01% of its construction land. The average urbanization rate of eastern China was 64.56%, which was higher than the national rate of 58.52%; Shanghai had the highest urbanization rate in the country (87.70%). The high density of the population in this region has increased the demand for farmland, housing, and energy [52]. The extraction of environmental resources and the discharge of pollutants has had deleterious effects on the environment and has resulted in the loss of biodiversity and other ecosystem services, soil degradation, and the disruption of hydrological cycles [53]. Humans are constantly modifying the environment to accommodate their needs, yet this land-use change is also an important driver of human stress [54]. Over the past decades, China has experienced varying extents of urbanization. Intense urbanization improves social development in various ways but often creates substantial human pressures that could have negative effects on human welfare [55].

Human pressures in China have expanded over time. The main contributors to the HF model were construction land, areas of high population density, and road surroundings. From 2000–2017, China's population (1.27–1.40 billion, +0.6%/year), GDP (12.7–80.3 trillion, +31.0%/year), urbanization rate (36.0%–58.5%, +3.5%/year), farmland area (128.3–134.9 square kilometer, +0.3%/year), road area (2000–8000 square kilometer, +16.7%/year), livestock output (0.7–2.9 trillion, +16.5%/year) increased rapidly, which may be the reason that human pressure has increased by 13.6%. Human pressures from eastern, central, northeastern, and southwestern China have been increasing significantly over time, and the potential environmental implications caused by expanding human pressures associated with economic development require increased attention [56]. The control of these high-pressure areas is needed to relieve anthropogenically induced environmental damage.

4.2. CO₂ Emissions in China

Given China's large size and the heterogeneity in its economic development, lifestyles, resources, and economies vary among the provinces [57]. Eastern and northern China are the main contributors to CO₂ emissions and account for 45.39% of total emissions in China based on the 18-year average. The provinces of Shandong (2017 GDP: 1.12 trillion USD) and Jiangsu (2017 GDP: 1.38 trillion USD) in eastern China are two of the most developed regions in China and account for approximately 20% of the national total GDP. They also account for 15.71% of total CO₂ emissions given their large industrial areas and advanced technology. In contrast, the provinces of Inner Mongolia, Shanxi, and Hebei in northern China are less developed regions that account for only 7.86% of the country's GDP but 16.94% of its CO₂ emissions. Similar patterns were observed for northeastern and northwestern China.

CO₂ emissions continuously increased from 2000 to 2014 and declined in 2015–2017 by –5.52%, –3.10%, and –1.85% from the previous year, respectively. The economy of China has grown rapidly since its reform and opening in the 1970s. This economic expansion has led to the emission of a large amount of CO₂. From 2000 to 2017, China's GDP increased by 724.83% from 1.55 trillion US dollars (USD) to 12.80 trillion USD. Infrastructure construction and energy consumption have been the major drivers of the rapid growth of China's economy and emissions since 2002 [56]. The economy relies on carbon-intensive industries such as thermal power generation, steel, cement, and vehicle production. Due to increased greenhouse gas emissions, a tight energy supply, and severe air pollution, the government of China has begun to implement a series of strategies to conserve energy and mitigate emissions. The 11th and 12th Five-Year Plan (2006–2015) strategies have reduced emissions of CO₂ and coal by 3 billion tons and 1.4 billion tons, respectively [58]. From 2015–2017, the effect of slowing population growth (1.38–1.40 billion, +0.5%/year) and the optimization of industrial structure (2014, +4% CO₂) may result in a decrease in carbon emissions reduction and air pollution improvement. According to the report of the Netherlands Environmental Assessment Agency (PBL), China's carbon emissions increased by only 0.9% in 2014, despite its economic growth of 7% [59]. The slowdown in economic growth, coupled with the shift to cleaner energy and the reduction of energy intensive manufacturing has reduced the energy intensity of the country's economy. Control of the growth of CO₂ emissions in economically underdeveloped regions such as northwestern China will require the restructuring and upgrading of industry and industrial technology, respectively.

4.3. Impacts of Human Pressures on CO₂ Emissions

The CO₂ emissions per unit of economic output and per capita in the northern provinces are mostly higher than the national average, which indicates that economic development in northern China disproportionately contributes to CO₂ emissions compared with other regions of the country (Figure 8). For example, Shanghai led the country in CO₂ emissions per capita in 2000 (7.91 t per capita⁻¹), while Ningxia was first in 2017 (25.16 t per capita⁻¹) and has seen its CO₂ emissions increase more than three-fold since 2000 (5.97 t per capita⁻¹). The population and GDP are higher, and industrial development is more advanced in Shanghai compared with Ningxia. Several factors have caused the CO₂ emissions per capita to stabilize (2017, Shanghai, 7.95 t per capita⁻¹). The mismatch in the increase in GDP and technology levels in western China is an important factor affecting CO₂ emissions per capita. The high degree of economic development and the large human population in eastern China are the main reasons for the expansion of the high–high clustering area of CO₂ emissions. However, increasing energy consumption in northern China is the main factor underlying the emergence of the high–high clustering region [60]. Three northern provinces were among the top five emitters in 2000 (Figure 8a); in 2017 however, the top five emitters in the country were all northern provinces (Figure 8b). The carbon intensity (CO₂ per unit of GDP) of China decreased from 2000 to 2017 due to changes in economic development. The less economically developed provinces were mainly located in northern and western China. The carbon intensity of these regions mostly exceeded the national average in 2000 (49.86 t per USD⁻¹) (Figure 8c) and 2017 (17.00 t per USD⁻¹) (Figure 8d). Heavy industries are central to the economies of the northern provinces, and these products are mainly exported to other provinces [61]. Such provinces do not have adequate human resources to upgrade their technologies and equipment, and the economies of these provinces are mainly based on energy-intensive industries, such as mining, metals, electricity, and chemical products; consequently, the resource use efficiency of these provinces is low, and their greenhouse gas emissions are high [56]. China's economy is largely dependent on primary energy resources, and these resources are mainly located in less developed regions. Technology transfer and optimization of the industrial structure are important for reducing CO₂ emissions in less developed regions [62].

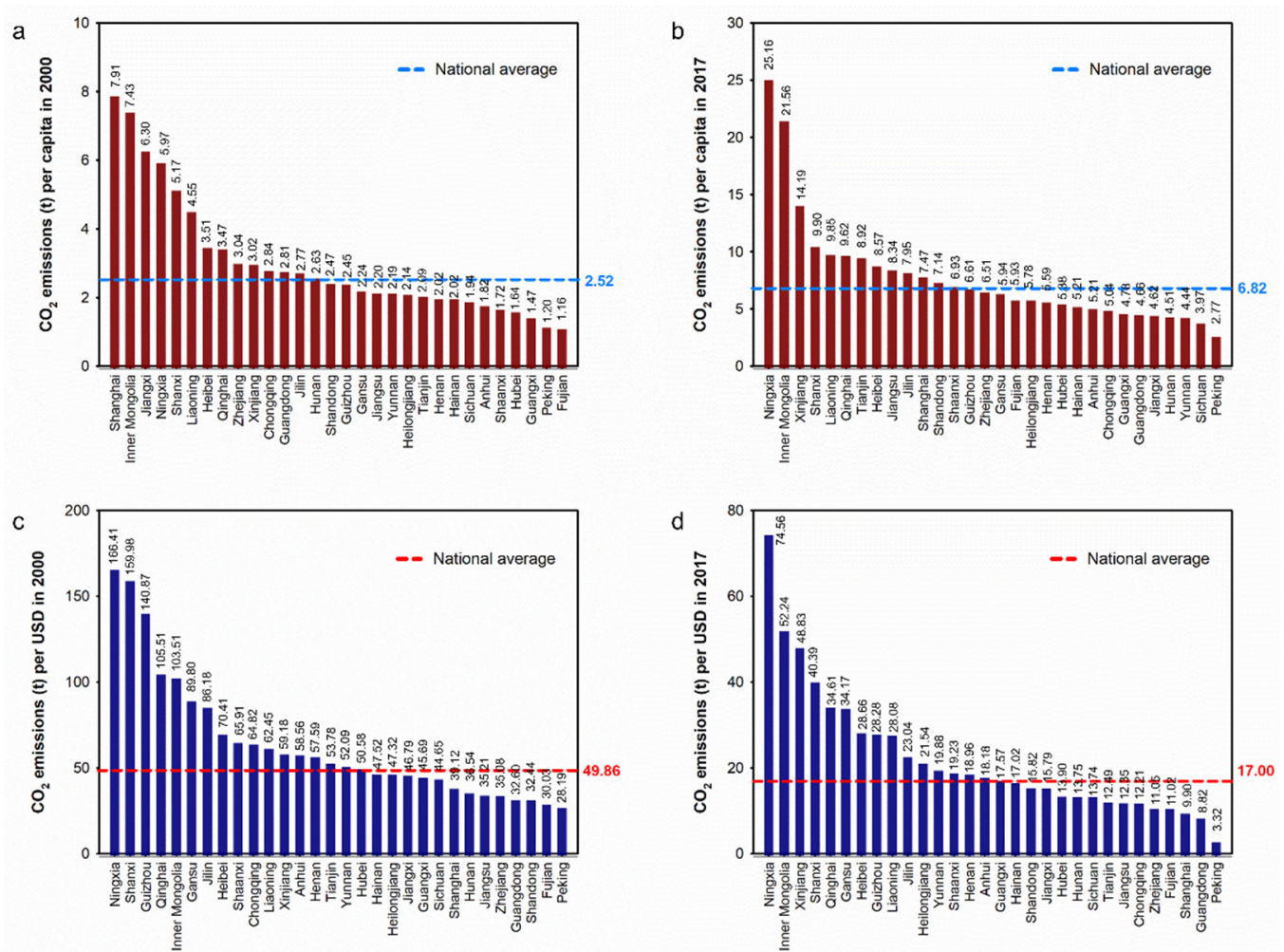


Figure 8. CO₂ emissions per capita (t) in (a) 2000 and (b) 2017 in each provincial administrative unit. CO₂ emissions per USD (g) in (c) 2000 and (d) 2017. The dotted line indicates the national average.

As increased human pressures lead to increased CO₂ emissions, spatial heterogeneity in the strength of human pressures leads to spatial heterogeneity in CO₂ emissions. Northern China is the main region contributing to increases in CO₂ emissions in response to human pressures. Thermal power generation is a major source of CO₂ emissions but an unsustainable form of energy generation in eastern and southern China. Northern China is rich in coal resources. The integrated development of coal and electricity has become widespread in China, and most thermal power generation units are concentrated in Inner Mongolia, Shanxi, and Xinjiang provinces [63], which has made northern China a major source of CO₂ emissions. Therefore, special effort is needed to control the intensity of human activities and greenhouse gas emissions in these regions. Modifications of the energy structure would be an effective approach to the reduction of CO₂ emissions in these regions [64]. Controlling the rate of increase in human pressures can also contribute to the mitigation of CO₂ emissions. There is thus a need to reduce the effect of human pressures on the environment, especially the deleterious effects of the human population, land-use structure, and urban construction.

One of the most important factors driving the reduction in energy consumption and CO₂ emissions in China is the increase in high-quality development. Photovoltaic (PV) power is considered one of the most promising low-carbon energy generation approaches in China [65]. By the end of 2015, the cumulative installed capacity of PV generation reached approximately 43 million kilowatts, which made China the largest solar power producer in the world [66]. By the end of 2030, the installed PV capacity will reach 100 million

kilowatts, which is equivalent to building more than 30 fewer large coal power plants. At the Climate Ambition Summit in 2020, China's national leader proposed that the total installed capacity of wind and solar power would reach more than 1.2 billion kilowatts by 2030. Ultra-high voltage (UHV) technology makes significant contributions to the reduction of CO₂ emissions [67]. China has been committed to developing UHV technology for many years. As of 2019, more than 20 UHV transmission lines have been built in China [68]. In addition, the Chinese government has been vigorously promoting the use of new energy vehicles (NEVs). Annual sales of NEVs were 1.367 million in 2020, which is more than 160 times the number of NEVs sold in 2011 (8159) [69]. Direct policy support has promoted the rapid development of China's NEV market and has made large contributions to energy saving and emission reductions.

5. Conclusions

Along with the development of economy and the acceleration of urbanization, human pressure on the environment is increasing. An understanding of the spatiotemporal dynamics in CO₂ emissions under changing human pressures is essential for designing sustainable environmental strategies. Our findings have implications for the development of mitigation policies for CO₂ emissions by local governments. The main findings and policy implications are manifold. First, carbon emissions in China are still on the rise; there is thus a need to strengthen the implementation of CO₂ reduction measures. Second, CO₂ emissions in China are unevenly distributed spatially (generally higher in the south and east and lower in the north and west), indicating that the government needs to optimize the regional allocation of energy. Third, increased human pressures have increased the amount of CO₂ emissions, and northern China is the main region driving this pattern. Given that little can be done to alter the current economic trend, the impacts of human activities on CO₂ emissions can be reduced by optimizing land use, population density, and grazing density. Fourth, CO₂ emissions associated with anthropogenic activities are decreasing. High-quality development measures and strong national macroeconomic control instruments are needed to achieve China's goal of carbon neutrality. We believe that China is on track to meet its carbon reduction commitments on time.

Remote sensing technology has expanded peoples' abilities to understand their living environment, and has the advantages of qualitative accuracy, large observation range, high spatial resolution, simple acquisition, and strong data consistency. However, government-based datasets have certain advantages in terms of quantitative analysis. Our next goal is to conduct a bottom-up carbon footprint coupled with remote sensing data and government-based datasets for an analysis of the impact of human activities on carbon emissions.

Supplementary Materials: The following supporting information can be downloaded at: <https://www.mdpi.com/article/10.3390/rs15020426/s1>. Figure S1. Analytical scope of CO₂ emissions including (a) spatial distribution diagram of the monitoring area at the county level and (b) spatial distribution of regions in China used for estimating CO₂ emissions. Figure S2. Annual CO₂ emissions by seven regions in China. Figure S3. Annual CO₂ emissions (g) per USD in China during 2000–2017. National average is 1.45 g CO₂ per USD based the 18-year period. Figure S4. Average CO₂ emissions in China in each provincial administrative unit. Table S1. Spatio-temporal characteristics of the human footprints in China. Table S2. Spatio-temporal characteristics of CO₂ emissions.

Author Contributions: Y.L. and W.M. conceived the study and wrote the paper. L.J. and Y.Z. completed some of the statistical analyses. Q.H. and Y.W. provided suggestions for manuscript revision. Y.B. provided feedback on various drafts of the manuscript. All authors have read and agreed to the published version of the manuscript.

Funding: This work was supported by the National Natural Science Foundation of China (No. 31971477; No. 42177057), the Key Laboratory of Algal Biology, Institute of Hydrobiology, Chinese Academy of Sciences (202205), Taiyuan University of Science and Technology Introduction of Talent Start-up Fund (2020051), and Incentive Fund for Outstanding Doctors Working in Shanxi (20212071).

Data Availability Statement: All the original data can be obtained from given data sources. The full dataset, including the spatio-temporal maps of CO₂ emissions and human footprint index used in this study is available. All datasets generated during this study are available from the corresponding author on reasonable request.

Conflicts of Interest: The authors declare that they have no known competing financial interest or personal relationships that could have influenced the work reported in this paper.

References

1. Corlett, R.T. The anthropocene concept in ecology and conservation. *Trends Ecol. Evol.* **2015**, *30*, 36–41. [CrossRef] [PubMed]
2. Watson, E.J.; Venter, O. Mapping the continuum of humanity's footprint on land. *One Earth* **2019**, *1*, 175–180. [CrossRef]
3. Zhang, L.; Xiong, L.; Li, J.; Huang, X. Long-term changes of nutrients and biocenoses indicating the anthropogenic influences on ecosystem in Jiaozhou Bay and Daya Bay, China. *Mar. Pollut. Bull.* **2021**, *168*, 112406. [CrossRef] [PubMed]
4. Grizzetti, B.; Pistocchi, A.; Liqueste, C.; Udias, A.; Bouraoui, F.; van de Bund, W. Human pressures and ecological status of European rivers. *Sci. Rep.* **2017**, *7*, 205. [PubMed]
5. Tilman, D.; Lehman, C. Human-caused environmental change: Impacts on plant diversity and evolution. *Proc. Natl. Acad. Sci. USA* **2001**, *98*, 5433–5440. [CrossRef]
6. Marques, A.; Martins, I.S.; Kastner, T.; Plutzer, C.; Theurl, M.C.; Eisenmenger, N.; Huijbregts, M.A.J.; Wood, R.; Stadler, K.; Bruckner, M.; et al. Increasing impacts of land use on biodiversity and carbon sequestration driven by population and economic growth. *Nat. Ecol. Evol.* **2019**, *3*, 628–637.
7. Zandalinas, S.I.; Fritschi, F.B.; Mittler, R. Global warming, climate change, and environmental pollution: Recipe for a multifactorial stress combination disaster. *Trends Plant Sci.* **2021**, *26*, 588–599. [CrossRef]
8. Mazdiyasi, O.; AghaKouchak, A. Substantial increase in concurrent droughts and heatwaves in the United States. *Proc. Natl. Acad. Sci. USA* **2015**, *112*, 11484–11489.
9. Noyes, P.D.; McElwee, M.; Miller, H.D.; Clark, B.W.; Van Tiem, L.A.; Walcott, K.C.; Erwin, K.N.; Levin, E.D. The toxicology of climate change: Environmental contaminants in a warming world. *Environ. Int.* **2009**, *35*, 971–986. [CrossRef]
10. du Pont, Y.R.; Meinshausen, M. Warming assessment of the bottom-up Paris Agreement emissions pledges. *Nat. Commun.* **2018**, *9*, 4810.
11. Editorials. Accesses Net-zero carbon pledges must be meaningful to avert climate disaster. *Nature* **2021**, *592*, 8. [CrossRef]
12. FAO (Food and Agriculture Organization of the United Nations). FAOSTAT. 2019. Available online: <http://faostat.fao.org/> (accessed on 1 January 2022).
13. Raupach, M.R.; Marland, G.; Ciais, P.; Le Quéré, C.; Canadell, J.G.; Klepper, G.; Field, C.B. Global and regional drivers of accelerating CO₂ emissions. *Proc. Natl. Acad. Sci. USA* **2007**, *104*, 10288–10293. [CrossRef]
14. Ibisch, P.L.; Hoffmann, M.T.; Kreft, S.; Pe'er, G.; Kati, V.; Biber-Freudenberger, L.; DellaSala, D.A.; Vale, M.M.; Hobson, P.R.; Selva, N. A global map of roadless areas and their conservation status. *Science* **2016**, *354*, 1423–1427. [CrossRef]
15. Harris, N.L.; Brown, S.; Hagen, S.C.; Saatchi, S.S.; Petrova, S.; Salas, W.; Hansen, M.C.; Potapov, P.V.; Lotsch, A. Baseline map of carbon emissions from deforestation in tropical regions. *Science* **2012**, *336*, 1573–1576. [CrossRef]
16. Haddad, N.M.; Brudvig, L.A.; Clobert, J.; Davies, K.F.; Gonzalez, A.; Holt, R.D.; Lovejoy, T.E.; Sexton, J.O.; Austin, M.P.; Collins, C.D.; et al. Habitat fragmentation and its lasting impact on Earth's ecosystems. *Sci. Adv.* **2015**, *1*, e1500052. [CrossRef]
17. Henders, S.; Persson, U.M.; Kastner, T. Trading forests: Land-use change and carbon emissions embodied in production and exports of forest-risk commodities. *Environ. Res. Lett.* **2015**, *10*, 125012. [CrossRef]
18. McGowan, P.J.K. Mapping the terrestrial human footprint. *Nature* **2016**, *537*, 172–173. [CrossRef]
19. Mi, Z.; Wei, Y.-M.; Wang, B.; Meng, J.; Liu, Z.; Shan, Y.; Liu, J.; Guan, D. Socioeconomic impact assessment of China's CO₂ emissions peak prior to 2030. *J. Clean. Prod.* **2017**, *142*, 2227–2236. [CrossRef]
20. Pflugmann, F.; Blasio, N.D. The geopolitics of renewable hydrogen in low-carbon energy markets. *Geopolit. Hist. Int. Relat.* **2020**, *12*, 9–44.
21. Li, X.; Huang, C.; Zhan, S.; Wu, Y. The carbon emission reduction effect of city cluster—Evidence from the Yangtze River Economic Belt in China. *Energies* **2022**, *15*, 6210. [CrossRef]
22. Labzovskii, L.D.; Mak, H.W.L.; Kenea, S.T.; Rhee, J.S.; Lashkari, A.; Li, S.; Goo, T.Y.; Oh, Y.S.; Byun, Y.H. What can we learn about effectiveness of carbon reduction policies from interannual variability of fossil fuel CO₂ emissions in East Asia? *Environ. Sci. Policy* **2019**, *96*, 132–140. [CrossRef]
23. Sanderson, E.W.; Jaiteh, M.; Levy, M.A.; Redford, K.H.; Wannebo, A.V.; Woolmer, G. The human footprint and the last of the wild. *Bioscience* **2002**, *52*, 172–173. [CrossRef]
24. Venter, O.; Sanderson, E.W.; Magrath, A.; Allan, J.R.; Beher, J.; Jones, K.R.; Possingham, H.P.; Laurance, W.F.; Wood, P.; Fekete, B.M.; et al. Sixteen years of change in the global terrestrial human footprint and implications for biodiversity conservation. *Nat. Commun.* **2016**, *7*, 12558. [CrossRef] [PubMed]
25. Halpern, B.S.; Walbridge, S.; Selkoe, K.A.; Kappel, C.V.; Micheli, F.; D'Agrosa, C.; Bruno, J.F.; Casey, K.S.; Ebert, C.; Fox, H.E.; et al. A global map of human impact on marine ecosystems. *Science* **2008**, *319*, 948–952. [CrossRef] [PubMed]

26. Mammides, C. A global assessment of the human pressure on the world's lakes. *Global Environ. Chang.* **2020**, *63*, 102084. [[CrossRef](#)]
27. Peters, G.; Andrew, R.; Boden, T.; Canadell, J.G.; Ciais, P.; Le Quééré, C.; Marland, G.; Raupach, M.R.; Wilson, C. The challenge to keep global warming below 2 °C. *Nat. Clim. Chang.* **2012**, *2*, 2–4. [[CrossRef](#)]
28. Chiu, C.-C.; Château, P.-A.; Lin, H.-J.; Chang, Y.-C. Modeling the impacts of coastal land use changes on regional carbon balance in the Chiku coastal zone, Taiwan. *Land Use Policy* **2019**, *87*, 104079. [[CrossRef](#)]
29. Doney, S.C. The Growing Human Footprint on Coastal and Open-Ocean Biogeochemistry. *Science* **2010**, *5985*, 1512–1516. [[CrossRef](#)]
30. Findell, K.L.; Berg, A.; Gentine, P.; Krasting, J.P.; Lintner, B.R.; Malyshev, S.; Santanello, J.A., Jr.; Shevliakova, E. The impact of anthropogenic land use and land cover change on regional climate extremes. *Nat. Commun.* **2017**, *8*, 989. [[CrossRef](#)]
31. Havlík, P.; Valin, H.; Herrero, M.; Obersteiner, M.; Schmid, E.; Rufino, M.C.; Mosnier, A.; Thornton, P.K.; Böttcher, H.; Conant, R.T.; et al. Climate change mitigation through livestock system transitions. *Proc. Natl. Acad. Sci. USA* **2014**, *111*, 3709–3714. [[CrossRef](#)]
32. Hong, C.; Burney, J.A.; Pongratz, J.; Nabel, J.E.M.S.; Mueller, N.D.; Jackson, R.B.; Davis, S.J. Global and regional drivers of land-use emissions in 1961–2017. *Nature* **2021**, *589*, 554–561. [[CrossRef](#)]
33. Houghton, R.A.; House, J.I.; Pongratz, J.; Van Der Werf, G.R.; DeFries, R.S.; Hansen, M.C.; Le Quééré, C.; Ramankutty, N. Carbon emissions from land use and land-cover change. *Biogeosciences* **2012**, *9*, 5125–5142. [[CrossRef](#)]
34. Lai, L.; Huang, X.; Yang, H.; Chuai, X.; Zhang, M.; Zhong, T.; Chen, Z.; Chen, Y.; Wang, X.; Thompson, J.R. Carbon emissions from land-use change and management in China between 1990 and 2010. *Sci. Adv.* **2016**, *2*, e1601063. [[CrossRef](#)]
35. Din, S.U.; Mak, H.W.L. Retrieval of land-use/land cover change (LUCC) maps and urban expansion dynamics of Hyderabad, Pakistan via Landsat Datasets and support vector machine framework. *Remote Sens.* **2021**, *13*, 3337. [[CrossRef](#)]
36. Arshad, S.; Kazmi, J.H.; Fatima, M.; Khan, N. Change detection of land cover/land use dynamics in arid region of Bahawalpur District, Pakistan. *Appl. Geomat.* **2022**, *14*, 387–403. [[CrossRef](#)]
37. Meng, X.; Han, J. Roads, economy, population density, and CO₂: A city-scaled causality analysis. *Resour. Conserv. Recy.* **2016**, *128*, 508–515. [[CrossRef](#)]
38. Yeboah, G.; de Albuquerque, J.P.; Troilo, R.; Tregonning, G.; Perera, S.; Ahmed, S.; Ajisola, M.; Alam, O.; Aujla, N.; Azam, S.; et al. Analysis of Openstreetmap data quality at different stages of a participatory mapping process: Evidence from Slums in Africa and Asia. *ISPRS Int. J. Geo-Inf.* **2021**, *10*, 265. [[CrossRef](#)]
39. Sugar, L.; Kennedy, C.; Leman, E. Greenhouse gas emissions from Chinese cities. *J. Ind. Ecol.* **2012**, *16*, 552–563. [[CrossRef](#)]
40. Achour, H.; Belloumi, M. Investigating the causal relationship between transport infrastructure, transport energy consumption and economic growth in Tunisia. *Renew. Sustain. Energy Rev.* **2016**, *56*, 988–998. [[CrossRef](#)]
41. Wang, X.; Meng, X.; Long, Y. Projecting 1 km-grid population distributions from 2020 to 2100 globally under shared socioeconomic pathways. *Sci. Data* **2022**, *9*, 563. [[CrossRef](#)]
42. Huang, R.; Lv, G.; Chen, M.; Zhu, Z. CO₂ emissions embodied in trade: Evidence for Hong Kong SAR. *J. Clean. Prod.* **2019**, *239*, 117918. [[CrossRef](#)]
43. Da, W.; Xu, R.; Wang, Y.; Wang, Y.; Liu, Y.; Yao, T. Responses of CO₂, CH₄ and N₂O fluxes to livestock enclosure in an alpine steppe on the Tibetan Plateau, China. *Plant Soil* **2012**, *359*, 45–55.
44. Gaughan, A.E.; Oda, T.; Sorichetta, A.; Stevens, F.R.; Bondarenko, M.; Bun, R.; Krauser, L.; Yetman, G.; Nghiem, S.V. Evaluating nighttime lights and population distribution as proxies for mapping anthropogenic CO₂ emission in Vietnam, Cambodia and Laos. *Environ. Res. Commun.* **2019**, *1*, 091006. [[CrossRef](#)] [[PubMed](#)]
45. Shi, K.; Shen, J.; Wu, Y.; Liu, S.; Li, L. Carbon dioxide (CO₂) emissions from the service industry, traffic, and secondary industry as revealed by the remotely sensed nighttime light data. *Int. J. Digit. Earth* **2021**, *14*, 1514–1527. [[CrossRef](#)]
46. Bennett, M.M.; Smith, L.C. Advances in using multitemporal night-time lights satellite imagery to detect, estimate, and monitor socioeconomic dynamics. *Remote Sens. Environ.* **2017**, *192*, 176–197. [[CrossRef](#)]
47. Chen, J.; Gao, M.; Cheng, S.; Hou, W.; Song, M.; Liu, X.; Liu, Y.; Shan, Y. County-level CO₂ emissions and sequestration in China during 1997–2017. *Sci. Data* **2020**, *7*, 391. [[CrossRef](#)]
48. Zhang, Y.; Lyu, M.; Yang, P.; Lai, D.Y.; Tong, C.; Zhao, G.; Li, L.; Zhang, Y.; Yang, H. Spatial variations in CO₂ fluxes in a subtropical coastal reservoir of Southeast China were related to urbanization and land-use types. *J. Environ. Sci.* **2021**, *109*, 206–218. [[CrossRef](#)]
49. Krivoruchko, K.; Gribov, A.; Krause, E. Multivariate areal interpolation for continuous and count data. *Procedia Environ. Sci.* **2011**, *3*, 14–19. [[CrossRef](#)]
50. Pyšek, P.; Jarošík, V.; Hulme, P.E.; Kühn, I.; Wild, J.; Arianoutsou, M.; Bacher, S.; Chiron, F.; Didžiulis, V.; Essl, F.; et al. Disentangling the role of environmental and human pressures on biological invasions across Europe. *Proc. Natl. Acad. Sci. USA* **2010**, *107*, 12157–12162. [[CrossRef](#)]
51. Meng, J.; Mi, Z.; Guan, D.; Li, J.; Tao, S.; Li, Y.; Feng, K.; Liu, J.; Liu, Z.; Wang, X.; et al. The rise of south–south trade and its effect on global CO₂ emissions. *Nat. Commun.* **2018**, *9*, 1871. [[CrossRef](#)]
52. West, P.C.; Gerber, J.S.; Engstrom, P.M.; Mueller, N.D.; Brauman, K.A.; Carlson, K.M.; Cassidy, E.S.; Johnston, M.; MacDonald, G.K.; Ray, D.K.; et al. Leverage points for improving global food security and the environment. *Science* **2014**, *345*, 325–328. [[CrossRef](#)]

53. Bala, G.; Caldeira, K.; Wickett, M.; Phillips, T.J.; Lobell, D.B.; Delire, C.; Mirin, A. Combined climate and carbon cycle effects of large-scale deforestation. *Proc. Natl. Acad. Sci. USA* **2007**, *104*, 6550–6555. [[CrossRef](#)]
54. Hansis, E.; Davis, S.J.; Pongratz, J. Relevance of methodological choices for accounting of land use change carbon fluxes. *Glob. Biogeochem. Cycles* **2015**, *29*, 1230–1246. [[CrossRef](#)]
55. Shen, F.; Yang, L.; He, X.; Zhou, C.; Adams, J.M. Understanding the spatial-temporal variation of human footprint in Jiangsu Province, China, its anthropogenic and potential implications. *Sci. Rep.* **2020**, *10*, 13316. [[CrossRef](#)]
56. Liu, Z.; Geng, Y.; Lindner, S.; Guan, D. Uncovering China’s greenhouse gas emission from regional and sectoral perspectives. *Energy* **2012**, *45*, 1059–1068. [[CrossRef](#)]
57. Feng, K.; Hubacek, K.; Guan, D. Lifestyles, technology and CO₂ emissions in China: A regional comparative analysis. *Ecol. Econ.* **2009**, *69*, 145–154. [[CrossRef](#)]
58. Qin, H.; Huang, Q.; Zhang, Z.; Lu, Y.; Li, M.; Xu, L.; Chen, Z. Carbon dioxide emission driving factors analysis and policy implications of Chinese cities: Combining geographically weighted regression with two-step cluster. *Sci. Total Environ.* **2019**, *684*, 413–424. [[CrossRef](#)]
59. Olivier, J.G.; Schure, K.M.; Peters, J.A.H.W. *Trends in Global CO₂ and Total Greenhouse Gas Emissions Summary of the 2017 Report*; Netherlands Environmental Assessment Agency, PBL: The Hague, The Netherlands, 2019.
60. Gregg, J.S. China: Emissions pattern of the world leader in CO₂ emissions from fossil fuel consumption and cement production. *Geophys. Res. Lett.* **2008**, *35*, L08806. [[CrossRef](#)]
61. Liu, Z.; Liang, S.; Geng, Y.; Xue, B.; Xi, F.; Pan, Y.; Zhang, T.; Fujita, T. Features, trajectories and driving forces for energy-related GHG emissions from Chinese mega cities: The case of Beijing, Tianjin, Shanghai and Chongqing. *Energy* **2012**, *37*, 245–254. [[CrossRef](#)]
62. Liu, Z.; Davis, S.J.; Feng, K.; Hubacek, K.; Liang, S.; Anadon, L.D.; Chen, B.; Liu, J.; Yan, J.; Guan, D. Targeted opportunities to address the climate–trade dilemma in China. *Nat. Clim. Chang.* **2016**, *6*, 201–206. [[CrossRef](#)]
63. CSC (China State Council). *China’s 12th Five-Year Plan for Energy Development*; CSC: Beijing, China, 2012.
64. Moutinho, V.; Moreira, A.C.; Silva, P.M. The driving forces of change in energy related CO₂ emissions in Eastern, Western, Northern and Southern Europe: The LMDI approach to decomposition analysis. *Renew. Sust. Energ. Rev.* **2015**, *50*, 1485–1499. [[CrossRef](#)]
65. Adaye, K.; Pearre, N.; Swan, L. Contrasting distributed and centralized photovoltaic system performance using regionally distributed pyranometers. *Sol. Energy* **2018**, *160*, 1–9. [[CrossRef](#)]
66. Liu, F.; Lv, T. Assessment of geographical distribution of photovoltaic generation in China for a low carbon electricity transition. *J. Clean. Prod.* **2019**, *212*, 655–665. [[CrossRef](#)]
67. Wei, W.; Wu, X.; Li, J.; Jiang, X.; Zhang, P.; Zhou, S.; Zhu, H.; Liu, H.; Chen, H.; Guo, J.; et al. Ultra-high voltage network induced energy cost and carbon emissions. *J. Clean. Prod.* **2018**, *178*, 276–292. [[CrossRef](#)]
68. Li, Y.; Yi, B.-W.; Wang, Y. Can ultra-high voltage power transmission bring environmental and health benefits? an assessment in China. *J. Clean. Prod.* **2020**, *178*, 124296. [[CrossRef](#)]
69. Wang, X.; Huang, L.; Daim, T.; Li, X.; Li, Z. Evaluation of China’s new energy vehicle policy texts with quantitative and qualitative analysis. *Technol. Soc.* **2021**, *67*, 101770. [[CrossRef](#)]

Disclaimer/Publisher’s Note: The statements, opinions and data contained in all publications are solely those of the individual author(s) and contributor(s) and not of MDPI and/or the editor(s). MDPI and/or the editor(s) disclaim responsibility for any injury to people or property resulting from any ideas, methods, instructions or products referred to in the content.